

# Vesicle trafficking plays a novel role in erythroblast enucleation

Ganesan Keerthivasan,<sup>1</sup> Sara Small,<sup>1</sup> Hui Liu,<sup>2</sup> Amittha Wickrema,<sup>2</sup> and John D. Crispino<sup>1</sup>

<sup>1</sup>Division of Hematology/Oncology, Northwestern University, Chicago, IL; and <sup>2</sup>Department of Medicine, University of Chicago, Chicago, IL

**Enucleation of mammalian erythroblasts is a process whose mechanism is largely undefined. The prevailing model suggests that nuclear extrusion occurs via asymmetric cytokinesis. To test this hypothesis, we treated primary erythroblasts with inhibitors of cytokinesis, including blebbistatin, hesperadin, and nocodazole, and then assayed for enucleation. Although these agents inhibited cell-cycle progression and subsequent enucleation when added early in culture, they failed to block enucleation proper**

**when added to postmitotic cells. These results suggest that contraction of the actomyosin ring is not essential for nuclear expulsion. Next, by ultrastructural examination of primary erythroblasts, we observed an accumulation of vacuoles in the cytoplasm proximal to the extruding nucleus. This finding led us to hypothesize that vesicle trafficking contributes to erythroblast enucleation. Here, we show that chemical inhibitors of vesicle trafficking block enucleation of primary erythroblasts without affecting**

**differentiation, cell division, or apoptosis. Moreover, knock-down of clathrin inhibited the enucleation of late erythroblasts. In contrast, vacuolin-1, a small molecule that induces vacuole formation, increased the percentage of enucleated cells. Together, these results illustrate that vesicle trafficking, specifically the formation, movement, and subsequent coalescence of vacuoles at the junction of the nucleus and the cytoplasm, is a critical component of mammalian erythroblast enucleation. (*Blood*. 2010;116(17):3331-3340)**

## Introduction

Enucleation is the final step in erythropoiesis before mammalian red blood cells enter the peripheral blood. Although many studies have shown that actin is required for this process,<sup>1,2</sup> the precise mechanism that governs this form of cellular maturation remains unknown. One of the prevailing models posits that enucleation of erythroid cells, lens epithelia, and keratinocytes is driven by apoptosis.<sup>3</sup> However, several lines of evidence suggest that apoptosis is not involved in the final steps of red blood cell maturation. First, inhibitors of caspases fail to block enucleation of primary erythroblasts, and expelled nuclei do not show DNA degradation.<sup>2</sup> Second, enucleation is not accompanied by cleavage of major nuclear substructural proteins, such as nuclear lamins, NuMA, or splicing factors Sm and SC35.<sup>4</sup> Rather, it appears that caspase activation functions in an earlier step of erythropoiesis, likely during the transition from pronormoblasts to basophilic normoblasts.<sup>5,6</sup>

Another model proposes that enucleation is a form of asymmetric cytokinesis. This hypothesis was first discussed in the 1960s and is based upon morphologic criteria developed from electron microscopic observations.<sup>7,8</sup> Recent data support this model. For example, the finding that the expelled nuclei have a thin rim of cytoplasm covered by intact plasma membrane<sup>2,9</sup> is consistent with a cell-division event, as opposed to simple exocytosis of the nucleus. Moreover, the identification of concentrated actin at the point of separation between the nucleus and nascent reticulocyte is similar to the contractile actomyosin ring that is characteristic of cytokinesis.<sup>1,10</sup> Although the presence of the actin cytoskeleton is required for enucleation,<sup>1,2,11</sup> its precise contribution to enucleation is unknown. Here, we investigated the role of cytokinesis in enucleation and discovered that cytokinesis is not required for

enucleation proper. Rather, erythroblast enucleation requires the formation, movement, and fusion of cytoplasmic endocytic vesicles.

## Methods

### Materials

Mouse monoclonal anticlathrin heavy chain (clone TD.1 from Covance) and mouse anti-HSC-70 (Santa Cruz Biotechnology) antibodies were used for Western blot assays. Syto 16, Syto 64, SytoX blue, SytoX red, and Transferrin AF-594 were purchased from Molecular Probes. Annexin V-Cy5 was purchased from BioVision. Blebbistatin, SU-6656, compound A5, MiTMAB, dynasore, vacuolin-1, *N*-benzyl-*p*-toluene sulphonamide (BTS), and 2,3-butanedione 2-monoxime (BDM) were purchased from Calbiochem EMD Biosciences, whereas nocodazole, cytochalasin D, sucrose, brefeldin A, and colchicine were purchased from Sigma-Aldrich. Monensin was generously provided by Dr Piers Nash (University of Chicago).

### Flow cytometry

All acquisitions were performed on an LSRII flow cytometer (Becton Dickinson). Data were analyzed using FlowJo software Version 8.8.6 (TreeStar).

### Enucleation assays of primary murine erythroblasts

Enucleation assays of primary murine spleen erythroblasts were performed as described by Yoshida et al.<sup>2</sup> For assays involving small molecule inhibitors of cytokinesis or vesicle trafficking, drugs were added at the start of the culture. After 5 hours, cells were collected and processed as previously described.<sup>2</sup> All animal studies were approved by the Northwestern University Animal Care and Use Committee.

Submitted March 29, 2010; accepted July 12, 2010. Prepublished online as *Blood* First Edition paper, July 19, 2010; DOI 10.1182/blood-2010-03-277426.

An Inside *Blood* analysis of this article appears at the front of this issue.

The online version of this article contains a data supplement.

The publication costs of this article were defrayed in part by page charge payment. Therefore, and solely to indicate this fact, this article is hereby marked "advertisement" in accordance with 18 USC section 1734.

© 2010 by The American Society of Hematology

For enucleation assays of fetal liver erythroblasts, cells were collected from E12.5-14.5 wild-type C57Bl/6 embryos and subjected to Ter119 depletion (StemCell Technologies) to remove mature erythroblasts and reticulocytes. Enucleation assays were then performed as previously described.<sup>11</sup> For assays involving small molecule inhibitors of cytokinesis or vesicle trafficking, drugs were added at either 24 or 38 hours of culture. Cells were collected after 48 hours of total incubation and stained, and the percentages of reticulocytes were quantified at 48 hours by gating on the Syto 64<sup>low</sup>- and Ter119-phycoerythrin-positive populations. The Student *t* test (paired, 2-tail distribution) was used to evaluate the statistical significance of the differences in enucleation. Cell-cycle progression and cell death were measured by flow cytometry of propidium iodide or annexin V-phycoerythrin and SytoX red staining, respectively. Note that dead cells were represented by both the SytoX red- and annexin V-positive gates.

Since dynasore is inhibited by the presence of serum proteins,<sup>12</sup> erythroblasts were washed in serum-free media several times before being plated in a serum-free media supplement ( $\alpha$ -minimal essential medium for spleen or Iscove modified Dulbecco medium for fetal liver assay, and 1% Nutridoma-SP [Roche Applied Science] and 2mM L-glutamine) with or without dynasore. Enucleation percentages were measured as described above.

### Transferrin uptake and live cell imaging in primary fetal liver erythroblasts

Fetal liver erythroblasts were cultured as described above (enucleation assays of primary murine erythroblasts) for 40 hours, washed, and then incubated for 20 minutes in serum-free media to enhance the uptake of fluorescently labeled transferrin. Next, MiTMAB, monensin, or solvent alone (100% ethanol) were added to the media at the indicated concentrations and incubated for 2 hours. Finally, transferrin AF-594 (5  $\mu$ g/mL) was added, and live cell images were acquired with a Nikon Eclipse C1Si scanning confocal microscope after 15 minutes.

### Enucleation assays of primary human erythroblasts

Human primary CD34<sup>+</sup> early hematopoietic cells were cultured in vitro in order to promote lineage commitment and differentiation into the erythroid lineage as previously described.<sup>13</sup> To knockdown the expression of clathrin, cells were transfected with 100nM small interfering RNA (siRNA) ON-TARGETplus SMARTpool siRNAs against clathrin light chain (L-004002-00; note that knocking down clathrin light chain results in a corresponding decrease in clathrin heavy chain<sup>14</sup>), or a nontargeting control siRNA (D-001810-10) on days 10 and 11 of culture with TransIT-TKO reagent (Mirus Bio). Lysates were prepared from cells on day 13 to evaluate the extent of protein knockdown. On day 14, 0.2 million cells were cytopun onto poly-L-lysine-coated slides (Sigma-Aldrich) and stained with benzidine and hematoxylin to visualize hemoglobin and nuclei, respectively. For enucleation assays with vesicle-trafficking inhibitors, day 13 cells were treated with drugs for 30 hours and placed on slides in the same way. Slides were viewed under a light microscope and scored in a blinded fashion for the total number of benzidine-positive cells and the number of enucleated erythrocytes. Between 100 and 200 cells were counted per field, and 4 adjacent fields of similar location in all slides were subjected to counting. Statistical significance was determined by the paired, 2-tailed Student *t* test.

### Hemoglobin estimation

The hemoglobin contents of primary mouse fetal liver erythroblasts cultured in the absence or presence of vesicle-trafficking inhibitors were quantified as previously described,<sup>15</sup> with minor modifications. After 38 hours of culture, erythroblasts were incubated with vesicle-trafficking inhibitors, washed twice with 1 $\times$  phosphate-buffered saline, and then resuspended in 0.5 mL of distilled water. The cells were then subjected to a cycle of freeze-thaw, centrifuged at 20 000g for 10 minutes, and 0.2 mL of the resultant cell lysates were transferred to 96-well plates in duplicates. Freshly prepared benzidine solution (20  $\mu$ L) and 30% (wt/wt) hydrogen

peroxide (8  $\mu$ L) were added to each well, and after a 5-minute incubation, plates were read using a BIO-TEK Synergy-HT (Bio-Tek Instruments), measuring the absorbance at 595 nm. A standard curve was generated by plating titrations of a freshly prepared hemoglobin solution (Sigma-Aldrich).

### Electron microscopy

Terminal erythroblasts derived from fetal liver progenitors after 48 hours of differentiation were subject to centrifugation and then fixed in 0.1M sodium cacodylate buffer (pH 7.4), 2% glutaraldehyde, and 2% paraformaldehyde solution overnight at 4°C. The pellets were then washed 3 $\times$  in 0.1M sodium cacodylate buffer (pH 7.4), fixed in 2% osmium in 0.1M sodium cacodylate (pH 7.4) for 1 hour, rinsed in distilled water, and prestained with uranyl acetate for 30 minutes. Cells were then washed with water and dehydrated by ethanol. After 3 changes of propylene oxide, cells were applied in a mixture of propylene oxide and Epon/Araldite (1:1 ratio) for 1 hour, embedded in Epon/Araldite resin, and placed in a 60°C oven overnight to polymerize. Uranyl acetate and lead citrate were used to stain the ultrathin sections, and images were acquired with a JEOL 1200EX electron microscope. Images were captured with a Gatan Ultrascan 4000SP camera and analyzed with GatanDigitalMicrograph software Version 1.4.3.

### MEL cell culture

Mouse erythroleukemia (MEL) cells were cultured in RPMI medium with 2mM L-glutamine, 10% fetal bovine serum, 100 U penicillin, and 100  $\mu$ g streptomycin. Staining of cells with Syto 16 and SytoX blue (Molecular Probes) or Syto 16 and annexin V-cy5 (BioVision) was performed as previously described.<sup>2</sup>

### Quantitative reverse transcription polymerase chain reaction

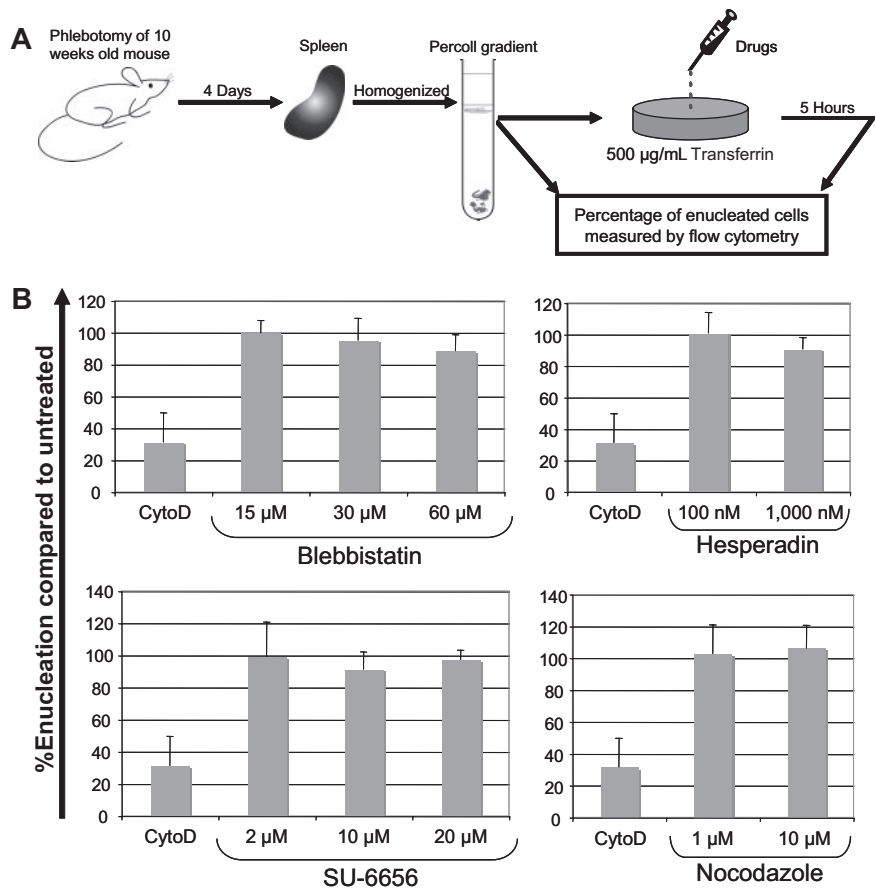
RNA was isolated from cells using TRIzol reagent (Invitrogen). cDNA was prepared using the SuperScript III (Invitrogen) cDNA preparation kit. Real-time polymerase chain reaction was performed by standard methods, and data were analyzed by the  $\Delta\Delta C(T)$  method. 18S RNA was used as the standard.

## Results

### Cytokinesis is not required for enucleation

To determine at what stage the characteristic events of cytokinesis, including the contractile actomyosin ring, are required for enucleation, we performed short-term (5-hour) ex vivo enucleation assays of primary murine erythroblasts in the presence of various chemical inhibitors of cytokinesis.<sup>16</sup> These drugs included blebbistatin, a nonmuscle myosin II ATPase inhibitor that prevents contraction of the actomyosin ring during cytokinesis, SU-6656, which disrupts cytokinesis by preventing the formation of the filipin ring, hesperadin, an aurora B kinase inhibitor, and nocodazole, a microtubule-stabilizing factor. For these assays, we collected spleens from wild-type phlebotomized mice, generated single-cell suspensions, and then separated cells on a Percoll gradient (Figure 1A). The resulting mononuclear cells, 40%-50% of which were CD71<sup>+</sup>/Ter119<sup>+</sup> erythroblasts, were incubated for 5 hours in the presence of drugs, stained with Syto16 and SytoX, and the degree of enucleation was evaluated by flow cytometry. We discovered that blebbistatin, hesperadin, SU-6656, and nocodazole all failed to inhibit enucleation, whereas cytochalasin D, an inhibitor of actin polymerization that is known to inhibit enucleation,<sup>1</sup> potently blocked this process (Figure 1B and supplemental Figure 1, available on the *Blood* Web site; see the Supplemental Materials link at the top of the online article). Although these cytokinesis inhibitors failed to block enucleation, similar doses of each

**Figure 1. Inhibitors of cytokinesis do not block enucleation of mouse spleen erythroblasts.** (A) Schematic showing the methodology of the short-term primary mouse spleen enucleation assay. Typically, between 12% and 18% of cells undergo enucleation in this short-term culture. (B) Results of enucleation assays performed in the presence of the cytokinesis inhibitors, blebbistatin, hesperadin, SU-6656, or nocodazole. The extent of enucleation was determined by quantifying the fractions of Syto 16-negative (permeable nucleic acid stain)/SytoX-negative (nonpermeable nucleic acid stain) cells by flow cytometry before and after a 5-hour incubation. The net percentage of enucleation was derived by taking the difference between the zero and 5-hour time points. Enucleation, compared with untreated, was calculated by multiplying  $100 \times$  ratio of the net percentage of enucleation of a drug-treated condition to the net percentage of enucleation of the corresponding solvent-control-treated condition. Cytochalasin D, a known inhibitor of enucleation, was included as a control for each experiment. Bars depict mean  $\pm$  standard deviation of 3 independent experiments.



potently inhibited cell-cycle progression of MEL cells (supplemental Figure 2). Based on the lack of an inhibitory effect on enucleation, we conclude that asymmetric cytokinesis is not the proximal mechanism of erythroblast enucleation.

Because other groups have reported that inhibitors of cytokinesis interfere with enucleation of erythroid cells, we next used an extended 48-hour murine model of enucleation that included an early phase of proliferation, followed by cell-cycle exit and subsequent enucleation (Figure 2A). Ter119-negative fetal liver erythroblasts isolated from mouse embryos were cultured *ex vivo* for 48 hours as previously described<sup>11</sup> and treated with inhibitors of cytokinesis at either 24 or 38 hours (Figure 2B). We discovered that the addition of blebbistatin or nocodazole potently blocked enucleation at the 24-hour time point, but had no effect when added at 38 hours. Analysis of the cell cycle of these cultured cells revealed that both drugs caused cell-cycle arrest and polyploidization when added at 24 hours, but not at 38 hours. These findings demonstrate that inhibitors of cytokinesis inhibit enucleation indirectly by blocking cell-cycle progression of proliferating early erythroblasts. Coupled with our data from the short-term assays (Figure 1B), these results lead us to conclude that cytokinesis is not the main driving force behind enucleation.

#### Inhibitors of vesicle trafficking block enucleation of murine erythroblasts

Next, to gain insights into the mechanism of enucleation, we performed electron microscopy of mouse fetal liver erythroblasts and analyzed the ultrastructural features of enucleating cells. Intriguingly, we observed an accumulation of vesicles and vacuoles proximal to the extruding nuclei (Figure 3A), consistent with

previous reports.<sup>17,18</sup> These findings led us to hypothesize that vesicle trafficking may be associated with, and/or required for, enucleation. To test this model, we evaluated the effect of a battery of small molecules, including MiTMAB, dynasore, monensin, A5, sucrose, and brefeldin A (BFA), each of which act on various aspects of the vesicle-trafficking pathway, on enucleation. MiTMAB<sup>19</sup> and dynasore<sup>20</sup> are dynamin inhibitors that prevent endocytosis. Monensin, a lipid-soluble Na<sup>+</sup> ionophore, disrupts the Na<sup>+</sup> and H<sup>+</sup> gradients across the trans-Golgi network (TGN), endosomes, and lysosomes, and causes an increase in intraluminal pH, thereby blocking their secretory function and impairing traffic between endosomes and lysosomes.<sup>21</sup> Compound A5 is a piperazine-phenylethanol derivative that specifically inhibits trafficking between TGN and endosomes that depend on AP-1-mediated, clathrin-coated vesicle formation.<sup>22</sup> Sucrose effectively inhibits clathrin-coated pit formation and thus blocks endocytosis.<sup>23</sup> BFA is a fungal metabolite that interacts with the sec7 domain of the large guanine nucleotide exchange factors (GEFs) GBF1 (Golgi-associated BFA-resistant), BIG1 (BFA-inhibited1), and BIG2 (BFA-inhibited2) and inhibits their action on Arf1-3 (class I ADP ribosylation factor) GTPases.<sup>24</sup> Thus, BFA blocks the endoplasmic reticulum (ER) to Golgi transport and post-TGN traffic to endosomes that depend on AP-1-GGA (Golgi-localized,  $\gamma$ -ear-containing, Arf-binding protein) recruitment.<sup>25</sup>

We assayed the effect of endocytic vesicle-trafficking inhibitors on the enucleation of 2 sources of primary murine erythroblasts: adult spleen and fetal liver erythroblasts. With respect to fetal liver erythroblasts, MiTMAB and dynasore potently interfered with enucleation, but had little effect on cell-cycle progression, cell viability, or differentiation (Figure 3 and supplemental Figure 3).

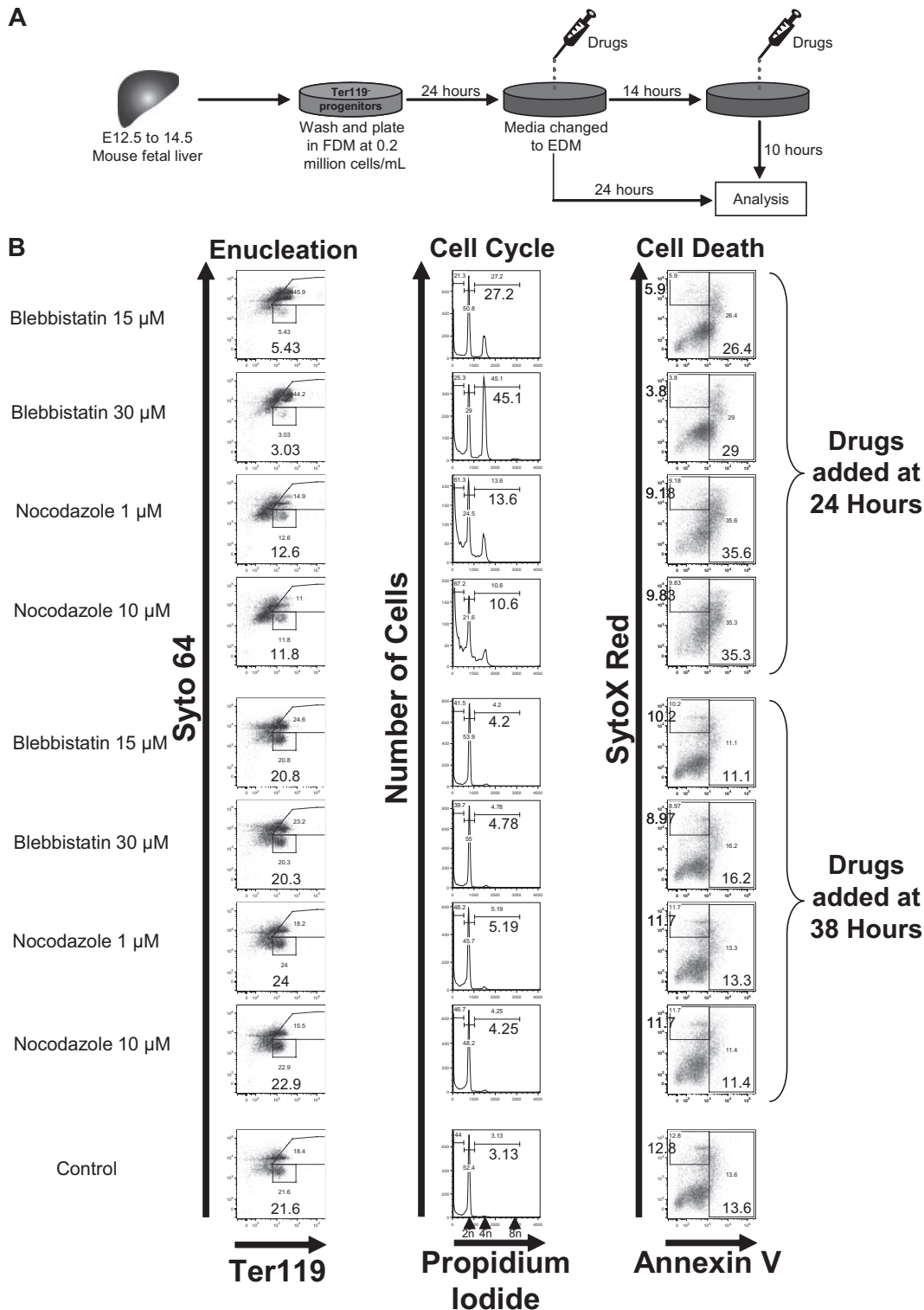


**Figure 2. Blebbistatin and nocodazole do not block enucleation of primary mouse fetal liver erythroblasts.** (A) Schematic of 48-hour fetal liver erythroblast enucleation assays. Typically, this system results in the accumulation of 15%-30% of enucleated cells. (B) Flow cytometric analysis of enucleation, cell cycle, and cell death of fetal liver cultures supplemented with blebbistatin or nocodazole at 24 or 38 hours. All flow cytometric analyses were performed after 48 hours of total culture time, and the profiles were shown. The percentage of reticulocytes after incubation were quantified by Syto 64/Ter119 staining, cell-cycle status by propidium iodide, cell death by annexin V/SyxoX red, and differentiation status by Ter119 positivity.

Similarly, monensin inhibited enucleation without affecting differentiation, but led to a similar extent of increased cell death at both 200nM and 1 $\mu$ M doses. Given that the block in enucleation was only observed with the higher dose, we conclude that the block in enucleation was not due to apoptosis. Similarly, MiTMAB, dyna-

sore, monensin, and sucrose blocked enucleation of primary splenic erythroblasts (Figure 4A). In contrast, BFA, which selectively targets ER to Golgi transport, and A5, which inhibits trafficking between the TGN and endosomes, failed to inhibit enucleation. These results demonstrate that intact endocytic vesicle trafficking



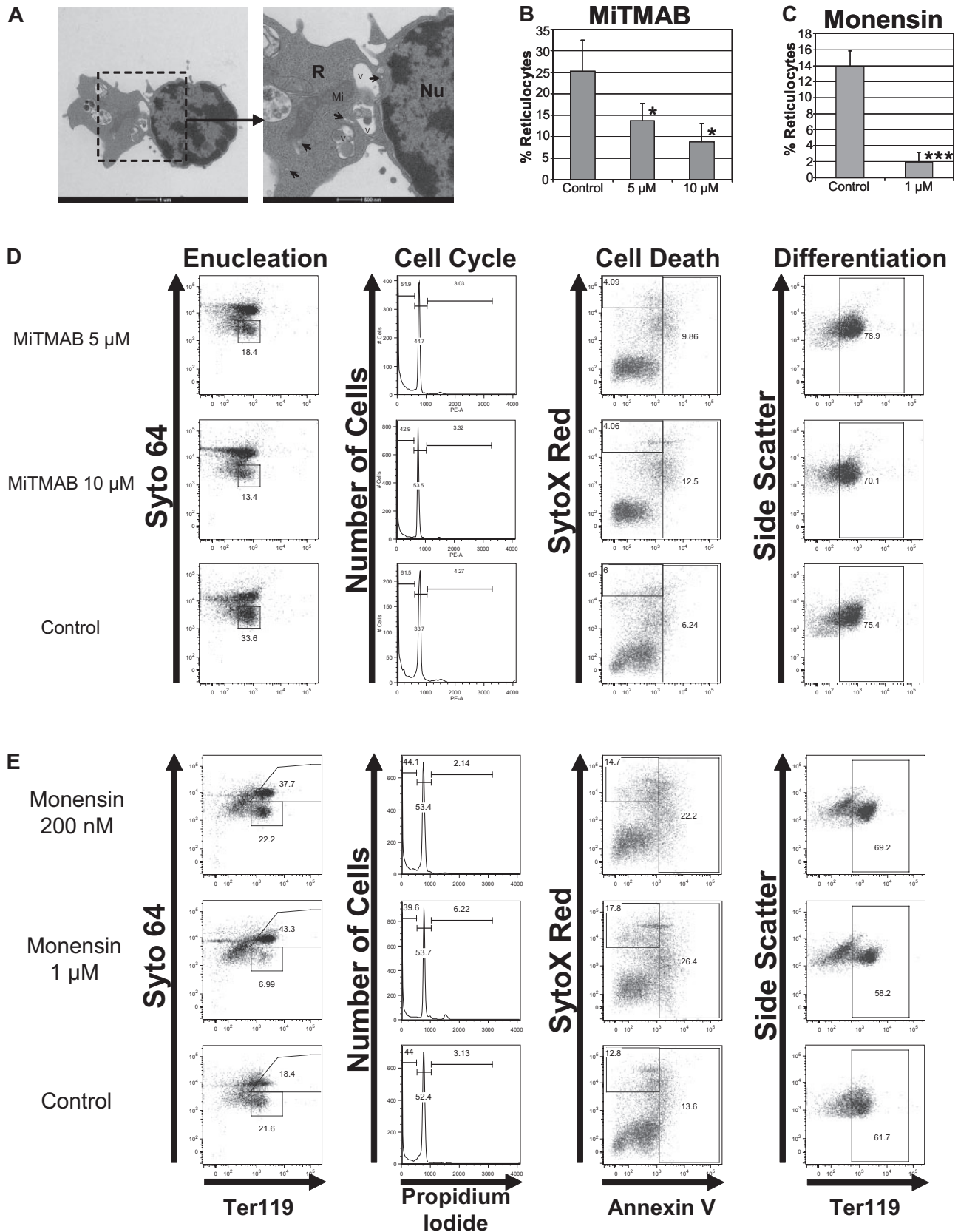


**Figure 3. Inhibitors of vesicle trafficking block enucleation of primary erythroblasts.** (A) Representative transmission electron microscopic image of mouse fetal liver erythroblasts cultured in vitro for 42 hours is shown. V indicates vacuoles; Mi, mitochondria; Nu, nucleus; R, incipient reticulocyte; and arrowheads, vesicles. Scale bar, 1  $\mu$ m. (B-C) Enucleation assays of primary mouse fetal liver erythroblasts were performed in the presence of MiTMAB, monensin, or their respective solvents. MiTMAB or monensin was added to culture at 38 hours, and flow cytometric analysis was performed after 48 hours of total culture time. Measured percentages of reticulocytes are shown as mean  $\pm$  standard deviation for 3 independent experiments. (D-E) Effect of MiTMAB (D) and monensin (E) on enucleation, cell cycle, viability, and differentiation when added to erythroblast cultures at 38 hours. Representative flow plots are shown.

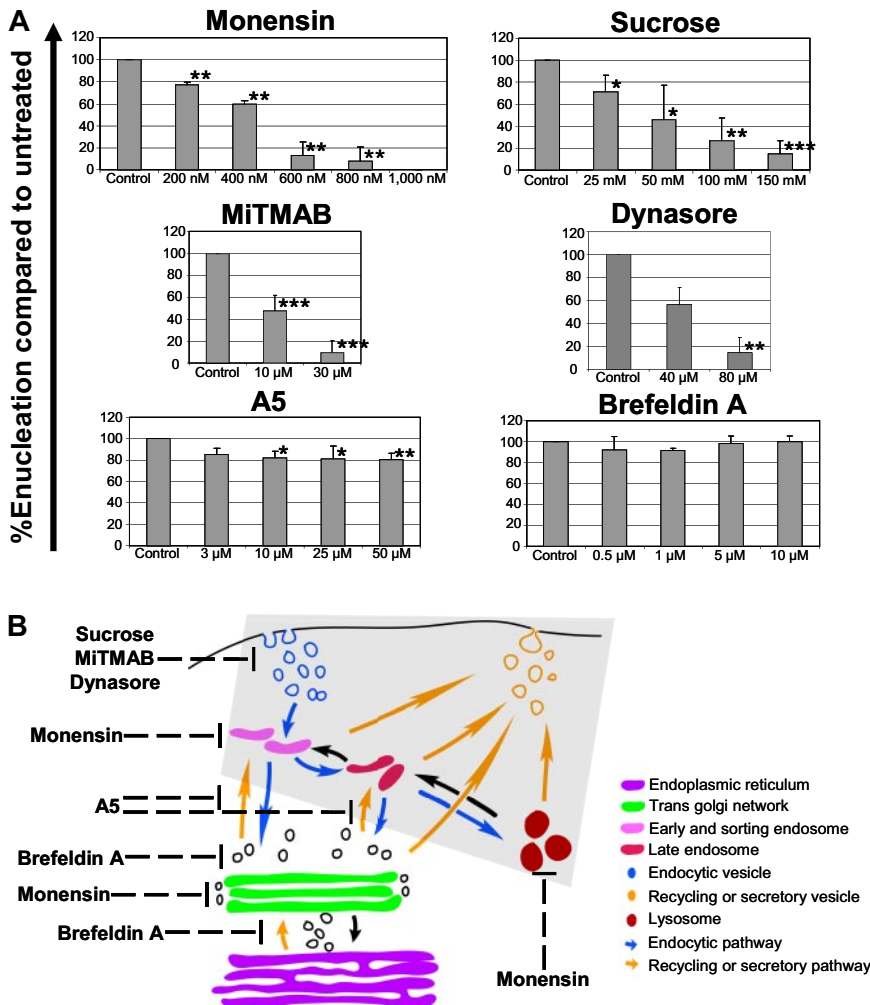


**Figure 4. Elucidation of vesicle-trafficking pathways that play a role in enucleation.** (A) Results of enucleation assays of primary mouse splenic erythroblasts in the presence of various inhibitors of vesicle trafficking. The enucleation efficiencies of erythroblasts in the presence of various concentrations of these drugs are shown as mean  $\pm$  standard deviation of 3 independent experiments. \* $P < .05$ , \*\* $P < .01$ , and \*\*\* $P < .001$ . (B) Schematic representation of various pathways of vesicle trafficking. Steps at which endocytic vesicle trafficking is disrupted by each of the inhibitors are depicted. The shaded region highlights the steps of vesicle trafficking that are required for enucleation.

and the endosome/lysosomal secretory pathways are selectively required for erythroblast enucleation, and further suggest that trafficking from the endoplasmic reticulum to the TGN and post-Golgi transport to endosomes are not essential for enucleation (Figure 4B). A role for vesicle trafficking in enucleation is further supported by our observation that BDM, a nonspecific inhibitor of myosin ATPase activity,<sup>26</sup> but not BTS, a specific inhibitor of muscle myosin II subfragment 1 actin-stimulated ATPase activity,<sup>27</sup> blocked enucleation (supplemental Figure 4). These data suggest that myosins V and VI, which participate in vesicle trafficking<sup>28-30</sup> and are blocked by BDM but not by BTS, may be required for enucleation.

Although we did not detect an effect of these drugs on differentiation, as assessed by Ter119 staining, we next investigated whether inhibition of vesicle trafficking would block accumulation of hemoglobin. We performed enucleation assays of primary murine fetal liver erythroblasts in the presence of vesicle-trafficking inhibitors and quantified both the extent of enucleation by flow cytometry and the degree of hemoglobin accumulation by a biochemical assay. We found that MiTMAB and monensin reduced enucleation, but failed to significantly affect hemoglobin accumulation (supplemental Figure 3). In particular, 10  $\mu$ M MiTMAB decreased enucleation by 90%, but only reduced the hemoglobin level by 10%. In contrast, dynasore caused a significant reduction in both hemoglobin accumulation and enucleation when used at both 40 and 80  $\mu$ M. However, the control reaction for dynasore, which included the use of a serum supplement in place of serum,

led to a 50% decline in hemoglobin concentration, but no difference in enucleation, compared with the serum-containing control. This argues against a simple correlation between enucleation efficiency and hemoglobin accumulation in vitro.

To determine how monensin treatment leads to a profound block in enucleation, we treated late stage primary mouse fetal liver erythroblasts with 1  $\mu$ M monensin for 10 hours and then observed the ultrastructure of the cells by electron microscopy. Whereas control solvent-treated cells harbored numerous cytoplasmic vacuoles, monensin-treated cells displayed few, if any, vacuoles (Figure 5A). Indeed, the presence of cytoplasmic vacuoles directly correlated with enucleation. To further confirm that MiTMAB and monensin function by interfering with endocytic vesicle trafficking, we monitored the uptake of labeled transferrin by mouse primary fetal liver erythroblasts in the absence or presence of these drugs. We found that both MiTMAB and monensin potently blocked the uptake of transferrin without inducing cell death (Figure 5B).

#### Enucleation of human erythroblasts is also disrupted by vesicle-trafficking inhibitors

To confirm that the essential role for vesicle trafficking extends beyond murine erythroblasts, we assayed the effect of MiTMAB and monensin on enucleation of primary human CD34<sup>+</sup> cells cultured under conditions to generate reticulocytes.<sup>13</sup> In this culture system, the majority of cells had reached the orthochromatic stage

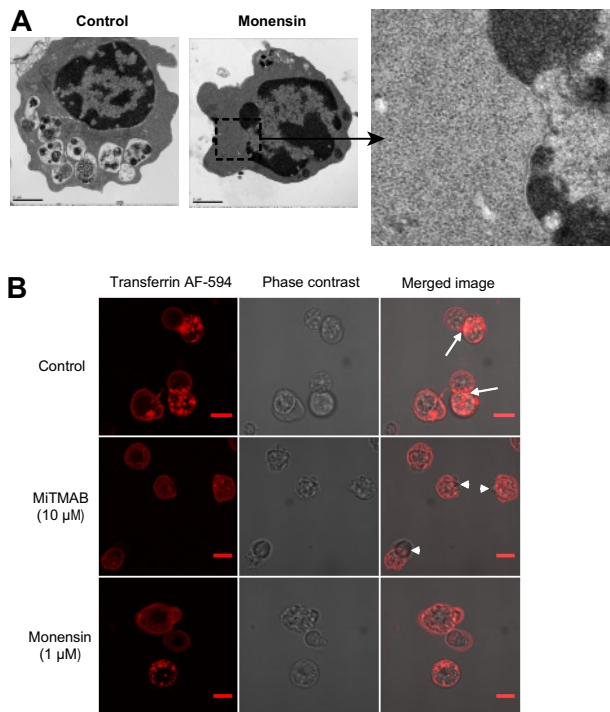


**Figure 5. Monensin blocks vacuole formation.** (A) Transmission electron microscopic images of mouse fetal liver erythroblasts cultured with  $1\ \mu\text{M}$  monensin added at 38 hours after start of culture along with control are shown. Scale bar,  $1\ \mu\text{m}$ . (B) The effect of MiTMAB or monensin on vesicular trafficking was evaluated by monitoring transferrin AF-594 uptake in mouse primary fetal liver erythroblasts in the absence or presence of  $10\ \mu\text{M}$  MiTMAB and  $1\ \mu\text{M}$  monensin. Live cell images were acquired with a Nikon Eclipse C1Si laser scanning confocal microscope with a  $100\times/1.40$  oil objective and were visualized with a 32 element multi-anode PMT detector. Images were processed using EZ-C1 Gold Version 3.8.0 and Image J Version 1.44a. Control cells displayed strong transferrin uptake, as evidenced by staining of cytoplasmic vesicles and vacuoles, with a striking alignment in the region between the nucleus and cytoplasm (arrow). In contrast, MiTMAB and monensin potently blocked transferrin uptake and disrupted the distribution of transferrin receptors on the plasma membrane along the nuclear side (arrowhead) of the cells. Scale bar,  $2\ \mu\text{m}$ .

by 10–12 days and had exited the cell cycle by day 12; by day 14, approximately 30%–40% of the cells had enucleated. MiTMAB and monensin were added to the cultures on day 13, incubated for 30 hours, and the effects on enucleation were quantified. Consistent with our murine data, we found that MiTMAB and monensin significantly blocked enucleation (supplemental Figure 5): in comparison to control cultures, which generated 37.5% reticulocytes,  $10\ \mu\text{M}$  MiTMAB and monensin ( $0.2\ \mu\text{M}$ ) led to 22.98% ( $P < .01$ ) and 26.2% ( $P < .05$ ) reticulocytes, respectively.

#### Clathrin-dependent endocytic vesicle trafficking plays an important role in enucleation

Having discovered that vesicle trafficking plays an important role in enucleation, we next asked whether the endocytosis during enucleation is clathrin- or caveolin-dependent. Primary human  $\text{CD}34^+$  cells cultured under conditions to generate reticulocytes<sup>13</sup> were harvested, and RNA (days 3, 7, 10, and 14) and protein lysates (days 3, 6, 8, 10, 13, and 16) were prepared. We found that clathrin increased from days 3 to 10 and remained elevated through day 16, whereas caveolin-1 was undetectable throughout erythroid development (supplemental Figure 6).

Next, to determine whether clathrin-mediated vesicle trafficking is required for enucleation, we used siRNA methodology to knock down its expression in orthochromatic erythroblasts derived

from primary human  $\text{CD}34^+$  cells. To achieve selective knock-down in late orthochromatic cells, we introduced siRNAs against clathrin, or a control siRNA, into the cells by transfection on days 10 and 11 of culture and then assayed the extent of protein knock down on day 13 and the effect on enucleation on day 14 (Figure 6). We discovered that knock down of clathrin heavy chain significantly reduced the extent of enucleation (25.5% vs 35.3%;  $P = .022$ ). Of note, the knock down of clathrin did not affect differentiation or survival of these primary cells (Figure 6C–D). These results demonstrate that clathrin contributes to erythroblast enucleation.

#### Increasing vacuole formation promotes enucleation

If enucleation is driven by accumulation of endocytic vesicles, then increased vacuole formation might enhance the process. To assay this, we treated primary murine fetal liver erythroblasts with vacuolin-1, which has been shown to promote the formation of enlarged vacuoles that are derived from the fusion of endosomes and lysosomes.<sup>31,32</sup> We discovered that vacuolin-1 conferred a dose-dependent increase in the enucleation of primary erythroblasts (Figure 7A) without affecting the cell cycle, cell death, or differentiation of erythroblasts (Figure 7B).

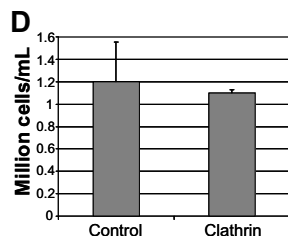
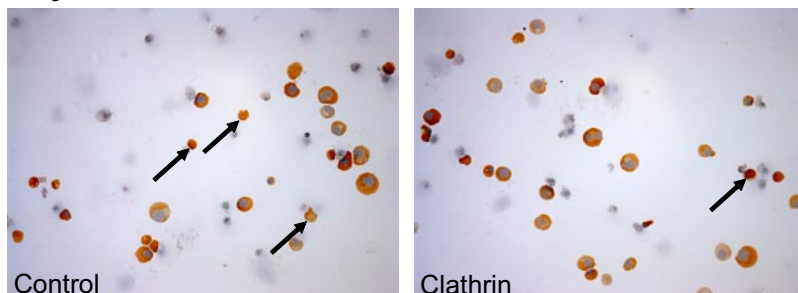
## Discussion

Enucleation is a late evolutionary event that provides mammalian reticulocytes with greater flexibility and increased oxygen-carrying capacity. Forty-year-old electron micrographs revealed that there is a marked similarity between enucleation and cytokinesis. In particular, erythroblast enucleation was accompanied by the appearance of centrioles, polysome disaggregation, and cytoplasmic protrusions, into one of which the nucleus penetrates.<sup>7,8</sup> Recent studies have confirmed that the process of nuclear expulsion is a cell-intrinsic phenomenon in which the extruded nucleus is encapsulated by a thin rim of cytoplasm.<sup>2</sup> After separation of the nucleus from the nascent reticulocyte, macrophages within the blood islands engulf expelled nuclei, which express phosphatidylserine on their surface. With respect to the mechanism of enucleation, the focus, of late, has been on investigating the role of the erythroid cytoskeleton and actin polymerization in this process. Elegant work by 2 groups has shown that RacGTPases contribute to enucleation by affecting the erythroid cytoskeleton and the formation of the contractile actin ring.<sup>11,33</sup> Despite the requirement for the formation of the contractile actin ring, our study provides strong evidence that other cellular events provide the driving force for enucleation. First, we show that blebbistatin, a selective nonmuscle myosin ATPase inhibitor that inhibits actomyosin ring contractility in cytokinesis,<sup>16</sup> does not block enucleation. Rather, the effect of the drug is to block cell-cycle progression during the earlier stages of terminal differentiation. Second, a src kinase inhibitor, SU-6656, which is known to prevent the filipin ring formation in cytokinesis,<sup>16</sup> also has no effect on enucleation. Third, we demonstrate that other inhibitors of cytokinesis, such as the aurora B kinase inhibitor, hesperadin, do not affect enucleation of primary erythroblasts. Finally, neither nocodazole nor colchicine, which stabilize or eliminate microtubule polymerization, respectively, affected enucleation (Figures 1B and 2B and supplemental Figure 7), suggesting the lack of a requirement for functional microtubule in enucleation.<sup>1,34</sup>

If endocytic vesicle trafficking, not cytokinesis, is the mechanism for enucleation, what explains the requirement for actin?

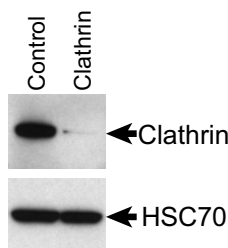
**A Day 14**

siRNA	Enucleated Cells (%)				P values (Compared to control)
	Expt1	Expt2	Expt3	Average	
Control	31.3	45.49	28.8	35.2	
Clathrin	18.9	38.16	19.3	25.5	0.022

**C Day 14**

Several lines of evidence suggest that actin is involved in vesicle trafficking. Actin is important for the formation of vesicles and for their initial movement away from the membrane.<sup>35,36</sup> Moreover, the actin cytoskeleton plays a critical role in the long range movements of vesicles that are mediated by myosins V and VI.<sup>37</sup> We propose that actin-dependent motor proteins, such as myosins V and VI, provide the force needed to move vesicles within the cytoplasm. Indeed, given that microtubules are not required for enucleation,<sup>1</sup> actin likely maintains the structure of the erythroblast and fuels the movement of intracellular organelles, including vesicles, endosomes, lysosomes, and vacuoles.

Our conclusion that enucleation is driven by the fusion of endocytic vesicles is supported by electron microscopic studies of enucleating canine erythroblasts, which highlighted an accumulation of vesicles within the cytoplasm of enucleating cells.<sup>17</sup> As enucleation proceeded, these vesicles coalesced to form dilated open spaces and irregular U-shaped channels in the vicinity of deep circumference of the nuclear envelope. These vesicles appeared to provide the plasma membranes needed to replace the area in which the nucleus had carried the original erythroblastic plasmalemma. Analysis of receptor-mediated endocytosis of transferrin in developing fetal liver erythroblasts further support our model that vesicles accumulate at the junction between the nucleus and nascent reticulocyte.<sup>18</sup> These studies showed that there was a perinuclear accumulation of transferrin in orthochromatic erythroid cells, which was followed by the localization of transferrin in the cytoplasm adjacent to the extruding nucleus.<sup>18</sup> Although the above-mentioned electron micrographs and transferrin uptake experiments depicted prominent features of vesicle trafficking in enucleating erythroblasts, no previous study has addressed the requirements for this process in enucleation.

**B****Figure 6. Knockdown of clathrin inhibits enucleation.**

(A) Human primary erythroid cells differentiated from CD34<sup>+</sup> cells were transfected on days 10 and 11 with siRNAs against clathrin light chain, or a control siRNA, and the effects on protein expression were determined by Western blot analysis on day 13 (B). On day 14, the cells were collected, washed, cytopun onto poly-L-lysine-coated slides and stained with benzidine and hematoxylin (C), and the percentage of enucleated cells were determined. The percentages of enucleated cells relative to the total number of benzidine-positive cells are shown for 3 independent experiments. Typically, this experimental system yields between 30% and 45% enucleated cells after 14 days. (B) Western blot showing knock-down efficiency of clathrin siRNA. Note that knocking down clathrin light chain decreases the levels of clathrin heavy chain, which is consistent with a previous report.<sup>14</sup> (C) Representative microscopic fields of benzidine and hematoxylin stained cytopins are shown. Orthochromatic erythroblasts and reticulocytes stained positive for benzidine (golden brown). Nuclei stained blue with hematoxylin. Arrows point to reticulocytes. Images were taken with a Leica DM 4000B microscope with 40 $\times$ 0.75 objective, visualized with a Leica DFC320 camera and analyzed by Adobe Photoshop 7.0. (D) The total number of live cells in both the siRNA treated conditions were counted by trypan blue exclusion on day 13, and the mean  $\pm$  standard deviation of 3 independent experiments were plotted.

Our proposed new model for erythroblast enucleation is as follows (Figure 7C and supplemental Video 1). First, by an unknown mechanism, the nucleus of a maturing orthochromatic erythroblast is moved to one side of the cell. Next, as the cell initiates the enucleation program, cytoplasmic vesicles move toward the nucleus, where they accumulate and fuse with plasma membrane to form U-shaped channels or coalescence to form large vesicles. As these vesicles fuse with one another along the periphery of the nascent reticulocyte, the 2 entities (ie, the nucleus and the reticulocyte) are separated from one another. Although we exclude major events of cytokinesis in this process, it is noteworthy that endocytic vesicle trafficking is postulated to provide membranes to complete cytokinesis in dividing cells.<sup>38,39</sup> Our model also reveals the source to satisfy the membrane requirements at the center during enucleation.

**Acknowledgments**

The authors thank Jonathan Licht, Gerd Blobel, Mitchell Weiss, Paul Ney, and James Palis for discussions and critical reading of the manuscript.

This work was supported by grants from National Institute of Diabetes and Digestive and Kidney Diseases (DK074693 to J.D.C.), National Cancer Institute (CA98550 to A.W.), the Giving Tree Foundation (to A.W.), and by the Katten Muchin Rosenman Travel Scholarship Award from the Robert H. Lurie Comprehensive Cancer Center of Northwestern University. J.D.C. is a Scholar of the Leukemia & Lymphoma Society. Imaging studies were performed at the Northwestern University Cell Imaging Facility, which is supported by National Cancer Institute Cancer Center Support Grant (P30 CA060553) awarded to the Robert H Lurie Comprehensive Cancer Center.



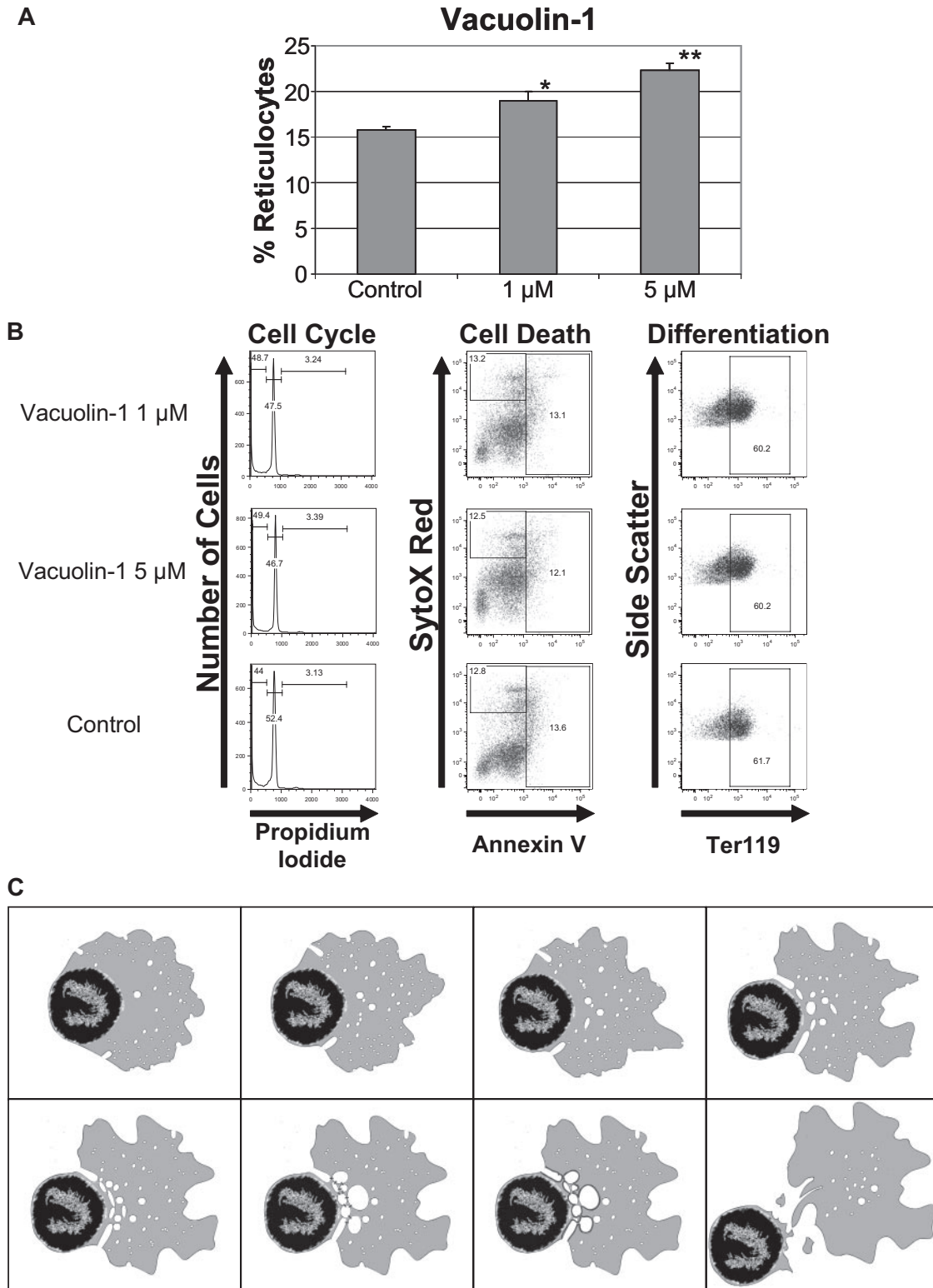


**Figure 7. Vacuolin-1 increases enucleation in mouse fetal liver erythroblasts.** (A) Effect of vacuolin-1 on enucleation of mouse fetal liver erythroblasts. The means  $\pm$  standard deviations for 3 independent experiments are shown. \* $P < .05$  and \*\* $P < .01$ . (B) Vacuolin-1 or its solvent were added to fetal liver enucleation assays at 38 hours and analyzed for effects on cell cycle, viability, and differentiation at 48 hours. Representative flow cytometric profiles are shown. (C) Model of erythroblast enucleation. An animated version is available as a supplemental video.

## Authorship

Contribution: G.K. designed and performed the experiments, interpreted the data, and contributed to writing the manuscript; S.S. and H.L. provided assistance with experiments; A.W. assisted with experimental design, data interpretation, and edited the manuscript;

and J.D.C. designed the experiments, interpreted the data, and contributed to writing the manuscript.

Conflict-of-interest disclosure: The authors declare no competing financial interests.

Correspondence: John D. Crispino, Division of Hematology/Oncology, Northwestern University, 303 East Superior St, Lurie 5-113, Chicago, IL 60611; e-mail: j-crispino@northwestern.edu.

## References

- Koury ST, Koury MJ, Bondurant MC. Cytoskeletal distribution and function during the maturation and enucleation of mammalian erythroblasts. *J Cell Biol*. 1989;109(6 Pt 1):3005-3013.
- Yoshida H, Kawane K, Koike M, Mori Y, Uchiyama Y, Nagata S. Phosphatidylserine-dependent engulfment by macrophages of nuclei from erythroid precursor cells. *Nature*. 2005;437(7059):754-758.
- Launay S, Hermine O, Fontenay M, Kroemer G, Solary E, Garrido C. Vital functions for lethal caspases. *Oncogene*. 2005;24(33):5137-5148.
- Krauss SW, Lo AJ, Short SA, Koury MJ, Mohandas N, Chasis JA. Nuclear substructure reorganization during late-stage erythropoiesis is selective and does not involve caspase cleavage of major nuclear substructural proteins. *Blood*. 2005;106(6):2200-2205.
- Kolbus A, Pilat S, Husak Z, et al. Raf-1 antagonizes erythroid differentiation by restraining caspase activation. *J Exp Med*. 2002;196(10):1347-1353.
- Carlisle GW, Smith DH, Wiedmann M. Caspase-3 has a nonapoptotic function in erythroid maturation. *Blood*. 2004;103(11):4310-4316.
- Skutelsky E, Danon D. An electron microscopic study of nuclear elimination from the late erythroblast. *J Cell Biol*. 1967;33(3):625-635.
- Skutelsky E, Danon D. Comparative study of nuclear expulsion from the late erythroblast and cytokinesis. *Exp Cell Res*. 1970;60(3):427-436.
- Hebiguchi M, Hirokawa M, Guo YM, et al. Dynamics of human erythroblast enucleation. *Int J Hematol*. 2008;88(5):498-507.
- Wickrema A, Koury ST, Dai CH, Krantz SB. Changes in cytoskeletal proteins and their mRNAs during maturation of human erythroid progenitor cells. *J Cell Physiol*. 1994;160(3):417-426.
- Ji P, Jayapal SR, Lodish HF. Enucleation of cultured mouse fetal erythroblasts requires Rac GTPases and mDia2. *Nat Cell Biol*. 2008;10(3):314-321.
- Kirchhausen T, Macia E, Pelish HE. Use of dynasore, the small molecule inhibitor of dynamin, in the regulation of endocytosis. *Methods Enzymol*. 2008;438:77-93.
- Kang JA, Zhou Y, Weis TL, et al. Osteopontin regulates actin cytoskeleton and contributes to cell proliferation in primary erythroblasts. *J Biol Chem*. 2008;283(11):6997-7006.
- Chu DS, Pishvaei B, Payne GS. The light chain subunit is required for clathrin function in *Saccharomyces cerevisiae*. *J Biol Chem*. 1996;271(51):33123-33130.
- Hafid-Medheb K, Augery-Bourget Y, Minatchy MN, Hanania N, Robert-Lezennes J. Bcl-XL is required for heme synthesis during the chemical induction of erythroid differentiation of murine erythroleukemia cells independently of its anti-apoptotic function. *Blood*. 2003;101(7):2575-2583.
- Ng MM, Chang F, Burgess DR. Movement of membrane domains and requirement of membrane signaling molecules for cytokinesis. *Dev Cell*. 2005;9(6):781-790.
- Simpson CF, Kling JM. The mechanism of denucleation in circulating erythroblasts. *J Cell Biol*. 1967;35(1):237-245.
- Iacopetta BJ, Morgan EH, Yeoh GC. Receptor-mediated endocytosis of transferrin by developing erythroid cells from the fetal rat liver. *J Histochem Cytochem*. 1983;31(2):336-344.
- Quan A, McGeachie AB, Keating DJ, et al. Myristyl trimethyl ammonium bromide and octadecyl trimethyl ammonium bromide are surface-active small molecule dynamin inhibitors that block endocytosis mediated by dynamin I or dynamin II. *Mol Pharmacol*. 2007;72(6):1425-1439.
- Macia E, Ehrlich M, Massol R, Boucrot E, Brunner K, Kirchhausen T. Dynasore, a cell-permeable inhibitor of dynamin. *Dev Cell*. 2006;10(6):839-850.
- Mollenhauer HH, Morre DJ, Rowe LD. Alteration of intracellular traffic by monensin; mechanism, specificity, and relationship to toxicity. *Biochim Biophys Acta*. 1990;1031(2):225-246.
- Duncan MC, Ho DG, Huang J, Jung ME, Payne GS. Composite synthetic lethal identification of membrane traffic inhibitors. *Proc Natl Acad Sci U S A*. 2007;104(15):6235-6240.
- Heuser JE, Anderson RG. Hypertonic media inhibit receptor-mediated endocytosis by blocking clathrin-coated pit formation. *J Cell Biol*. 1989;108(2):389-400.
- Duijsings D, Lanke KH, van Dooren SH, et al. Differential membrane association properties and regulation of class I and class II Arfs. *Traffic*. 2009;10(3):316-323.
- D'Souza-Schorey C, Chavrier P. ARF proteins: roles in membrane traffic and beyond. *Nat Rev Mol Cell Biol*. 2006;7(5):347-358.
- Forer A, Fabian L. Does 2,3-butanedione monoxime inhibit nonmuscle myosin? *Protoplasma*. 2005;225(1-2):1-4.
- Cheung A, Dantzig JA, Hollingworth S, et al. A small-molecule inhibitor of skeletal muscle myosin II. *Nat Cell Biol*. 2002;4(1):83-88.
- Mermall V, Post PL, Mooseker MS. Unconventional myosins in cell movement, membrane traffic, and signal transduction. *Science*. 1998;279(5350):527-533.
- Stachelek SJ, Kowalik TF, Farwell AP, Leonard JL. Myosin V plays an essential role in the thyroid hormone-dependent endocytosis of type II iodothyronine 5'-deiodinase. *J Biol Chem*. 2000;275(41):31701-31707.
- Buss F, Luzzio JP, Kendrick-Jones J. Myosin VI, an actin motor for membrane traffic and cell migration. *Traffic*. 2002;3(12):851-858.
- Cerny N, Feng Y, Yu A, et al. The small chemical vacuolin-1 inhibits Ca<sup>2+</sup>-dependent lysosomal exocytosis but not cell resealing. *EMBO Rep*. 2004;5(9):883-888.
- Huynh C, Andrews NW. The small chemical vacuolin-1 alters the morphology of lysosomes without inhibiting Ca<sup>2+</sup>-regulated exocytosis. *EMBO Rep*. 2005;6(9):843-847.
- Kalfa TA, Pushkaran S, Mohandas N, et al. Rac GTPases regulate the morphology and deformability of the erythrocyte cytoskeleton. *Blood*. 2006;108(12):3637-3645.
- Lemke C, Linss W. Remarks on the role of microtubules in enucleating normoblasts. *Anat Anz*. 1984;156(5):427-431.
- Merrifield CJ, Perais D, Zenisek D. Coupling between clathrin-coated-pit invagination, cortactin recruitment, and membrane scission observed in live cells. *Cell*. 2005;121(4):593-606.
- Le Clairinche C, Pauly BS, Zhang CX, Engqvist-Goldstein AE, Cunningham K, Drubin DG. A Hip1R-cortactin complex negatively regulates actin assembly associated with endocytosis. *EMBO J*. 2007;26(5):1199-1210.
- Soldati T, Schliwa M. Powering membrane traffic in endocytosis and recycling. *Nat Rev Mol Cell Biol*. 2006;7(12):897-908.
- Schweitzer JK, Burke EE, Goodson HV, D'Souza-Schorey C. Endocytosis resumes during late mitosis and is required for cytokinesis. *J Biol Chem*. 2005;280(50):41628-41635.
- Boucrot E, Kirchhausen T. Endosomal recycling controls plasma membrane area during mitosis. *Proc Natl Acad Sci U S A*. 2007;104(19):7939-7944.